

# Evaluation of economic disruptions from the 2016 Kumamoto Earthquake using a refined adaptive regional input-output model

Omar Issa<sup>1</sup>, Tinger Zhu<sup>2</sup>, Maryia Markhvida<sup>2</sup>, Rodrigo Costa<sup>3</sup>, and Jack W. Baker<sup>2</sup>

<sup>1</sup>Department of Civil and Environmental Engineering, Stanford University, Stanford, California, USA.

Email: oissa@stanford.edu

<sup>2</sup>Department of Civil and Environmental Engineering, Stanford University, Stanford, California, USA.

<sup>3</sup>Department of Systems Design Engineering, University of Waterloo, Waterloo, Ontario, Canada.

## ABSTRACT

The Adaptive Regional Input-Output (ARIO) model is popular for quantifying indirect economic losses, which stem from business and supply chain interruption. However, refining this model to study new contexts is challenging in its basic form due to low-resolution modeling of behavioral parameters and temporally static reconstruction rates. This paper presents a refined ARIO, or R-ARIO model that incorporates dynamic reconstruction rates, sector-level modeling of behavioral parameters, and explicit modeling of housing losses separately from productive capital losses. We perform a global variance-based sensitivity analysis to identify the most influential parameters on predicted indirect loss from the R-ARIO model. A case study application to the 2016 Kumamoto Earthquake Sequence isolates trends in housing and economic recovery, capturing temporal differences in reconstruction demand and uncertainty across economic indicators.

## INTRODUCTION

Indirect losses stemming from the disruptions in production and supply chains make up a substantial portion of post-disaster loss. The 1994 Northridge Earthquake, 2008 Wenchuan Earthquake, and 2011 Tohoku Earthquake generated 7.3, 124, and 211 billion U.S. dollars of indirect loss, respectively (Petak and Elahi 2000; Wu et al. 2012; MacKenzie et al. 2012). These losses, amounting to 17%, 35%, and 37% of the events' total post-disaster losses, illustrate that exclusive prediction of direct losses can significantly underestimate post-disaster impacts.

Several macroeconomic modeling tools have been developed to quantify post-disaster indirect loss across sectors in a regional economy. Input-output (I-O) models have been traditionally used to model such impacts.

27 These models leverage tables that characterize production inputs and outputs of each sector. However, a  
28 limitation of basic I-O models is that they cannot quantify supply-side shocks or capture business adaptation  
29 such as substitution or conservation of inputs by default (Koks et al. 2016; Galbusera and Giannopoulos 2018).  
30 As a result, I-O models tend to overestimate disaster impacts (Galbusera and Giannopoulos 2018; Hallegatte  
31 2014). A second approach is to use computable general equilibrium (CGE) models to simulate post-disaster  
32 impacts by estimating how shocks to the supply and demand of goods and services map to changes across  
33 economic indicators (e.g., Rose and Liao 2005). Unlike basic I-O models, they account for business  
34 adaptation behaviors, economies of scale, and nonlinear impact functions. However, without refinement,  
35 CGE models tend to overestimate resilient response by economic sectors, leading to underestimation of  
36 disaster impacts (Rose and Liao 2005; Botzen et al. 2019).

37 The Adaptive Regional Input-Output model (ARIO) extends basic I-O models by incorporating some  
38 CGE characteristics to consider changes in productive capacity due to productive capital losses and adaptive  
39 behaviors by individual sectors (Hallegatte 2008). Examples of adaptive behaviors include overproduction,  
40 which can be achieved through production recapture (e.g., overtime or extra shifts to compensate for lost  
41 production) or resource isolation (e.g., modifying operations to run without typical inputs). Both tactics have  
42 been demonstrated to be highly effective in various post-disaster contexts (Wein and Rose 2011; Haywired  
43 2019; Wei et al. 2020). The ARIO model has since been improved in Hallegatte (2014) to explicitly model  
44 inventories and production bottlenecks. The ARIO model was first used to predict economic recovery  
45 following Hurricane Katrina, and others have used it to evaluate climate change, earthquake, and flood  
46 impacts (Ranger et al. 2011; Zhang et al. 2017; Liu et al. 2023).

47 While the ARIO model and its applications enable the evaluation of post-disaster indirect loss, several  
48 barriers limit its use in new regions and contexts. First, the ARIO model assumes a constant, temporally  
49 static reconstruction rate for each sector, leading to identical reconstruction demands across all time steps  
50 until all productive capital has been reconstructed. While this rate can be modified, it cannot capture  
51 differences across sectors or time. Second, it does not have an explicit mechanism for handling housing  
52 losses, which often comprise a substantial portion of the total direct loss. Previous studies have assigned  
53 all housing reconstruction demand to the real estate sector (Hallegatte 2014; Markhvida and Baker 2023).  
54 This workaround captures housing-related reconstruction demands but distorts economic recovery for the  
55 real estate sector because it implies that housing is part of the productive capital of that sector. The extent of  
56 distortion will vary depending on the amount of damaged housing and productive capital in the real estate

57 sector.

58 Finally, ARIO model behavioral parameters are modeled at an economy-level resolution. These  
59 parameters—which characterize post-disaster adaptability, inventory, overproduction, and heterogeneity—  
60 significantly influence the predicted indirect loss. One consequence of low-resolution modeling is that a  
61 single change to one parameter must be applied to all sectors, regardless of inter-sector differences. Mod-  
62 elers wishing to select these parameters for new study regions must use a "one-size-fits-all" approach. As a  
63 result, several studies (e.g. [Ranger et al. 2011](#); [Zhang et al. 2017](#); [Wang et al. 2018](#); [Markhvida and Baker](#)  
64 [2023](#)) simply adopt the parameters used to model post-Katrina recovery introduced in [Hallegatte \(2008\)](#) or  
65 [Hallegatte \(2014\)](#), despite transferring them to a non-Katrina context. Furthermore, low-resolution modeling  
66 makes it more difficult to refine specific parameters since empirical evidence often exists at the sector or  
67 sector-category level, and it is not clear from sensitivity analyses which sectors contribute the most to the  
68 variance in the predicted ARIO output. Due to these challenges, past studies have not been able to perform  
69 sector-level sensitivity analyses or uncertainty quantification.

70 To address the abovementioned issues, this paper proposes the R-ARIO model to simulate post-disaster  
71 economic recovery. The R-ARIO model improves on previous iterations of the ARIO model by introducing  
72 (i) dynamic reconstruction rates based on sector-specific reconstruction time curves, (ii) explicit modeling  
73 of housing losses separate from productive capital losses, and (iii) sector-level modeling and uncertainty  
74 quantification of behavioral parameters. In addition, we propose the use of global sensitivity analyses  
75 to identify the most important behavioral parameters for further refinement. The R-ARIO model and the  
76 accompanying sensitivity analysis approach are demonstrated in a case study that explores economic recovery  
77 following the 2016 Kumamoto Earthquake. As part of the case study, we explore the influence of each model  
78 enhancement on the predicted indirect loss and illustrate how global sensitivity analyses can be used to  
79 prioritize future refinement of behavioral parameters.

## 80 **THE R-ARIO MODEL**

81 In this section, we provide an overview of the R-ARIO model and describe its inputs, outputs, and  
82 architecture. Subsections describe each model improvement in greater detail.

83 The R-ARIO model extends the work by [Hallegatte \(2014\)](#) in three ways:

- 84 1. Reconstruction demand is modeled dynamically throughout the recovery period using time-dependent,  
85 sector-specific reconstruction rates.

- 86 2. Housing losses are incorporated into the model explicitly and separately from productive capital  
 87 losses.
- 88 3. Behavioral parameter modeling is performed at the individual sector level to enable parameter  
 89 refinement that accounts for inter-sector differences and enables uncertainty quantification. We  
 90 propose a set of updated parameters that reflect these differences based on documented cases of  
 91 business adaptation.

92 Figure 1 illustrates the R-ARIO model workflow, which consists of three main steps.

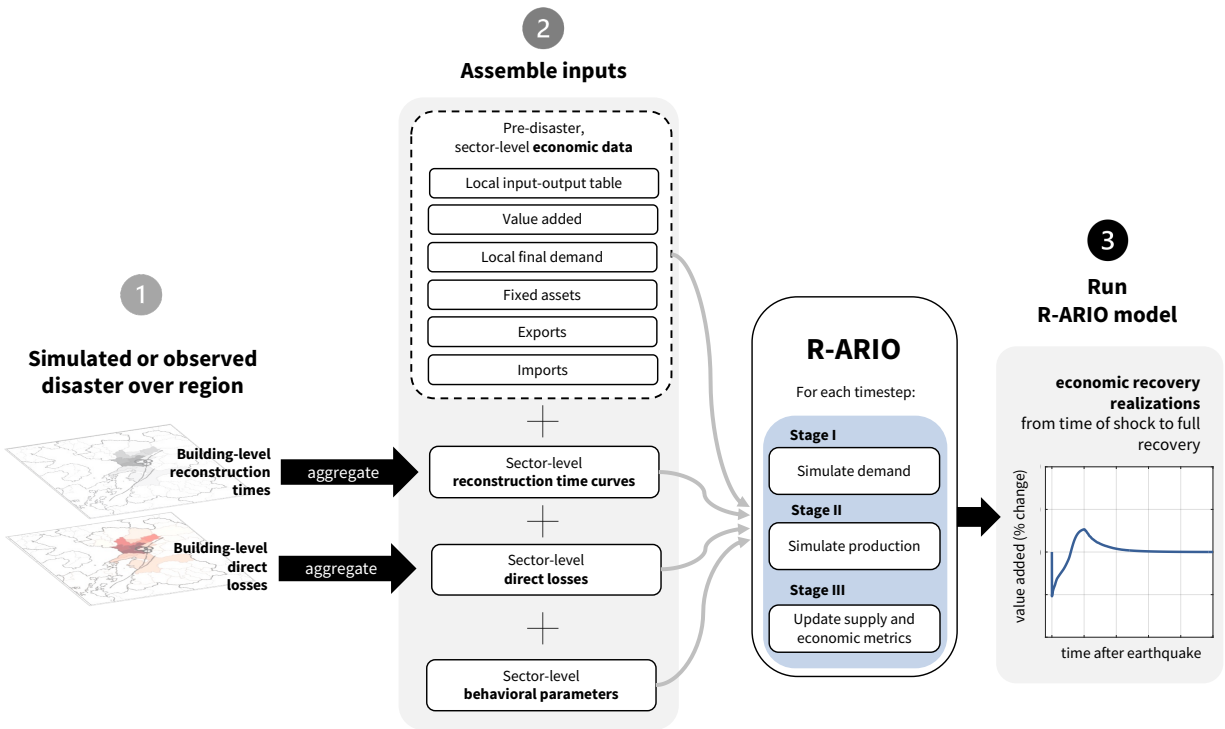


**Fig. 1.** General overview of the R-ARIO model workflow.

93 First, a study region and disaster are defined for the analysis. Disasters are based on observed past events  
 94 or hypothetical events (e.g., using simulation-based scenarios). The disaster is used to determine the spatial  
 95 extent of the study, and the amount of capital loss per sector resulting from the damage.

96 Next, input data specific to the regional economy (comprised of  $N_s$  sectors) is assembled. The required  
 97 data falls into four categories: pre-disaster economic activity (e.g., value added, exports), monetary losses  
 98 due to direct damage, reconstruction time curves, and behavioral parameters. These are detailed in Table 1.

99 Sector-level data encompasses a series of "baseline" inputs used to quantify steady-state economic

100 activity. The first of these inputs is the local input-output (I-O) table, a matrix representing the flow of  
101 goods and services exchanged between sectors in the defined economy, indicating how the outputs of one  
102 sector become an input for others. This table is used to derive input-output ratios that control the amount of  
103 inputs necessary to fulfill productive tasks. Next, value added and fixed assets are provided for each sector.  
104 Value added represents each sector's net contribution to the defined economy's output. It is calculated as  
105 the difference between a given sector's total output and the value of intermediate inputs it consumes from  
106 supplying sectors. Fixed assets represent the value of productive capital leveraged by each sector to produce  
107 goods and services. Fixed assets are assumed to equal the total replacement value of buildings within a given  
108 sector. Finally, exports, imports, and local demand are provided. Exports represent the value of goods and  
109 services produced by each sector within the defined economy that are sold outside the study region. Imports  
110 represent the value of goods and services produced by each sector outside the study region that are brought  
111 into the defined economy. Local final demand refers to the total demand for goods and services by final  
112 consumers.

113 Sector-level reconstruction time curves are time-dependent functions representing the reconstruction  
114 trajectory of damaged buildings within a specific sector. These inputs are used to determine sector-specific  
115 reconstruction rates of productive capital as part of the first enhancement in this study. User-provided  
116 reconstruction time curves only account for the time it takes to reconstruct buildings and do not include  
117 indirect delays that impede the start of repairs or slow work due to a lack of needed inputs. We describe the  
118 dynamic reconstruction rates below.

119 Sector-level direct losses are monetary losses directly attributed to damage from the disaster. These  
120 inputs control the loss of productive capital and the approximate drop in productive capacity, at the onset of  
121 the disaster for each sector.

122 Finally, sector-level behavioral parameters characterize adaptation and inventory mechanics of each  
123 sector following the disaster. Like the ARIO model, the R-ARIO model considers five behavioral parameters  
124 selected by the user to characterize the regional economy. These are discussed in greater detail later.

### 125 **Running the R-ARIO model**

126 At the beginning of each simulation, behavioral parameters are sampled from user-defined distributions  
127 for uncertainty quantification purposes. Each simulation tracks economic recovery at discrete time steps  
128 over a user-defined period. At each time step, a three-stage calculation (as shown in Figure 1) is performed

**TABLE 1.** Inputs to the R-ARIO model. Here,  $N_s$  represents the number of sectors in the defined economy, and  $(N_s + 1)$  represents the number of sectors, plus housing.  $N_{\text{step}}$  refers to the length of the time domain used as the x-axis of each recovery curve.

Input	Category	Size	Units	Differences in treatment (R-ARIO versus ARIO)
Local input-output table	Sector-level economic data	$N_s \times N_s$	Monetary value	None
Value added	Sector-level economic data	$N_s \times 1$	Monetary value	None
Exports	Sector-level economic data	$N_s \times 1$	Monetary value	None
Imports	Sector-level economic data	$N_s \times 1$	Monetary value	None
Local final demand	Sector-level economic data	$N_s \times 1$	Monetary value	None
Direct losses	Sector-level direct losses	$(N_s + 1) \times 1$	Monetary value	None
Reconstruction time curves	Sector-level reconstruction time curves	$(N_s + 1) \times N_{\text{step}}$	Unitless (Fraction of damaged capital reconstructed)	Used to determine time-dependant reconstruction time rates in R-ARIO. Not used in the ARIO model.
Behavioral parameters	Sector-level behavioral parameters	$N_s \times 5$	Varies by parameter	Modeled at the sector-level resolution in R-ARIO. Modeled at the economy-level in ARIO.

129 to estimate key economic metrics at the sector level.

130 *Stage I: Simulate demand*

131 Demand  $D_i(t)$  for each sector  $i$  is computed at each time step ( $t$ ) as the sum of inventory orders, local  
132 final demand, reconstruction demand due to damaged productive capital, and exports:

133 
$$D_i(t) = \sum_{\text{all } j} O_{j,i}(t) + C_i(t) + R_i(t) + E_i(t) \quad (1)$$

134

where:

$O_{j,i}(t)$  = Orders (intermediate consumption) from sector  $j$  to sector  $i$  at time  $t$

$C_i(t)$  = Local final demand to sector  $i$  at time  $t$

135

$R_i(t)$  = Reconstruction demand for sector  $i$  at time  $t$

$E_i(t)$  = Exports of sector  $i$  at time  $t$

136

At each time step, demand  $D_i(t)$  is satisfied by two sources: production and imports. If these two sources cannot fulfill demand, sectors begin proportionally rationing (using the ratio between production and demand at the current time step) across  $O_{j,i}(t)$ ,  $C_i(t)$ ,  $R_i(t)$ , and  $E_i(t)$ .

137

138

139

A key component in the calculation of demand  $D_i(t)$  is reconstruction demand  $R_i(t)$ . Fulfillment of reconstruction demand drives the restoration of productive capital over time.  $R_i(t)$  is estimated using

140

141

Equation 2:

142

$$R_i(t) = \sum_{\text{all } j} (RDM_{j,i}(t) \times \text{rate}_j(t)) \quad (2)$$

143

where:

$RDM_{i,j}(t)$  = Reconstruction demand from sector  $j$  to sector  $i$  at time  $t$ ;

144

$\text{rate}_j(t)$  = Rate of reconstruction of sector  $j$ 's productive assets at time  $t$

145

To take into account the time-dependent nature of reconstruction, the R-ARIO model introduces the term  $\text{rate}_j(t)$ , which represents the rate of reconstruction at the current time step, described further below.

146

147

*Stage II: Simulate production*

148

In the absence of supply-side constraints, the production of sector  $i$  would equal the demand for sector  $i$  at each time step. However, the R-ARIO model constrains the estimated production in two ways. It is first constrained by production capacity,  $P_i^{cap}(t)$ , when productive capital is insufficient to meet demand (e.g., in cases with significant direct damage to a sector). Production is also constrained by inventories. It is assumed that if inventories are lower than their required levels, then production is reduced.

150

151

152

The final value of production,  $P_i^a(t)$ , accounts for both the production capacity and inventory constraints.

153

Computing the value of  $P_i^a(t)$  follows three principal calculations. First, each sector's required inventory

154

levels  $S_{j,i}^r(t)$  are computed.  $S_{j,i}^r(t)$  represents the amount of input  $j$  necessary to meet the local production

155

level of sector  $i$  over the duration of inventory  $j$ , calculated as:

$$S_{j,i}^r(t) = \begin{cases} n_j \times (P_i^{cap}(t) - I_i(t)) \times A_{j,i}(t) & \text{if } D_i(t) > P_i^{cap}(t) \\ n_j \times D_i(t) \times \frac{P_i^{cap}(t) - I_i(t)}{P_i^{cap}(t)} \times A_{j,i}(t) & \text{if } D_i(t) \leq P_i^{cap}(t) \end{cases} \quad (3)$$

where:

$n_j$  = Target inventory level of supplying sector  $j$  in days of demand

$P_i^{cap}(t)$  = Production capacity of sector  $i$  at time  $t$

$I_i(t)$  = Imports of sector  $i$  at time  $t$

$A_{j,i}$  = I-O table coefficients (required units of input from sector  $j$  to produce unit of sector  $i$ )

Next, the maximum possible production of sector  $i$ ,  $P_{j,i}^{max}(t)$ , depends upon the actual inventory level of input  $j$ . If required inventory  $S_{j,i}^r(t)$  is not met, then the maximum possible production  $P_{j,i}^{max}(t)$  is reduced proportionally, taking into consideration inventory substitution effects (heterogeneity):

$$P_{j,i}^{max}(t) = \begin{cases} (P_i^{cap}(t) - I_i(t)) \times \min\left(1, \frac{S_{j,i}(t)}{\psi_j \times S_{j,i}(t)}\right) + I_i(t) & \text{if } D_i(t) > P_i^{cap}(t) \\ \min\left(D_i(t), D_i(t) \times \frac{P_i^{cap}(t) - I_i(t)}{P_i^{cap}(t)} \times \min\left(1, \frac{S_{j,i}(t)}{\psi_j \times S_{j,i}(t)}\right) + I_i(t)\right) & \text{if } D_i(t) \leq P_i^{cap}(t) \end{cases} \quad (4)$$

where:

$P_{j,i}^{max}(t)$  = Maximum production of sector  $j$  to sector  $i$

$S_{j,i}(t)$  = Actual inventory of input  $j$  for sector  $i$  at time  $t$

$S^r(j, i)(t)$  = Required inventory of sector  $j$  to sector  $i$  at time  $t$

$\psi_j$  = Production reduction parameter (heterogeneity) of sector  $j$

For each input sector  $j$ , if the current inventory is greater than or equal to  $S_{j,i}^r(t)$ , no sectoral constraints are applied. On the other hand, if a given sector cannot meet the required inventory, then its production is reduced using a ratio that considers heterogeneity in disaster losses and impacts. The top and bottom terms in Equation 4 account for the case in which the production capacity of sector  $i$  is insufficient and sufficient to fulfill demand, respectively.



171 Finally, the actual production  $P_i^a(t)$  is taken as the minimum of all sectoral constraints:

$$172 \quad P_i^a(t) = \min \left( P_{j,i}^{max}(t), \text{ for all } j \right) \quad (5)$$

173 *Stage III: Update supply and key economic metrics*

174 Demand and production are then used to update supply and calculate key economic metrics such as value  
175 added, which is calculated as production minus intermediate production and imports:

$$176 \quad VA_i(t) = P_i^a(t) - I_i(t) - \sum_{\text{all } j} A_{j,i} \times P_i^a(t) \quad (6)$$

177 where:

$VA_i(t)$  = Value added of sector  $i$  at time  $t$

178  $I_i(t)$  = Imports to sector  $i$  at time  $t$

$A_{j,i}$  = Coefficients of the I-O table

179 By repeating the calculations in Stages I through III across all sectors, value added, production, and  
180 unsatisfied demand can be tracked over time to produce economic recovery curves. Uncertainty across  
181 different economic metrics can be captured by rerunning the R-ARIO model using different behavioral  
182 parameter samplings. The resulting recovery curve ensembles for each sector, which consider uncertainty in  
183 the assumed behavioral parameters, are the final output of the R-ARIO model.

184 The following three sections cover the implementation of three R-ARIO enhancements in greater detail.

### 185 **Dynamic reconstruction rate**

186 Reconstruction demand plays a significant role in the economic recovery process, since it is a critical  
187 component of sector-specific demand  $D_i(t)$ , and drives the restoration of productive capital (and hence,  
188 production capacity) over time. Equation 2 indicates that the reconstruction demand is driven by the  
189 assumed rate of reconstruction,  $rate_j(t)$ .

190 Past iterations of the ARIO model (Hallegatte 2008; Hallegatte 2014) assume a constant value of  
191  $rate_j(t)$  for all timesteps. The original ARIO model assumed a constant half-year reconstruction time for  
192 all sectors, and hence, a rate of  $\frac{1}{0.5}$  throughout the recovery process. Markhvida and Baker (2023) extended  
193 this assumption to account for differences in reconstruction speed across sectors by using the time to 95%

194 reconstruction for sector  $j$  (i.e.,  $\tau_{j,95}$ ), based on sector-specific reconstruction times. While this allows for  
 195 differing reconstruction processes for each sector, it still employs a constant reconstruction rate equivalent  
 196 to  $\frac{1}{\tau_{j,95}}$  across the recovery period for each sector.

197 To account for temporal variations in this rate, the R-ARIO model leverages a "dynamic" reconstruction  
 198 rate for each sector  $j$  that is updated throughout a simulation based on reconstruction progress (Figure 2b).

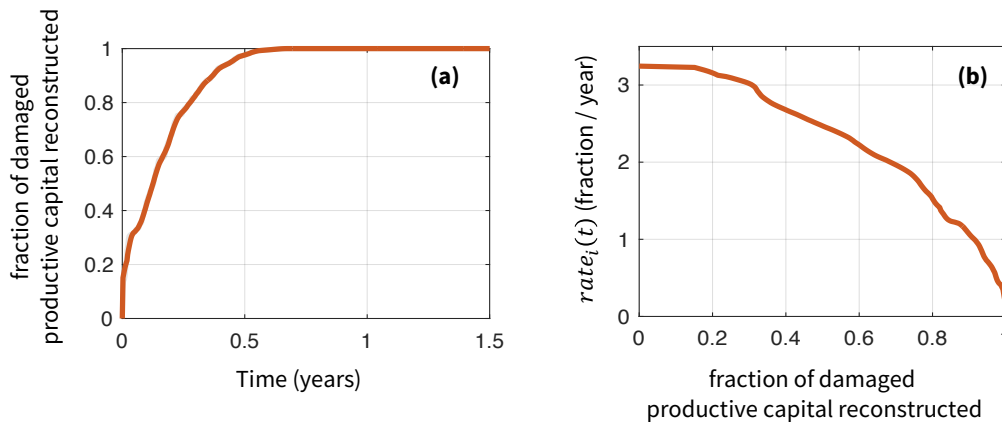


**Fig. 2.** In the R-ARIO model, the mapping between  $rate_j(t)$  and reconstruction progress (right) is developed using the user-provided reconstruction time curve for sector  $j$  (left).

199 For a given sector, the mapping between  $rate_j(t)$  and the fraction of damaged productive capital recon-  
 200 structed (Figure 2b) is derived using user-provided reconstruction time curves (Figure 2a). This is done by  
 201 taking the derivative of the reconstruction time curve with respect to time and then mapping it directly to the  
 202 fraction of damaged productive capital reconstructed.

### 203 **Explicit consideration of housing losses**

204 Housing damage can produce a significant portion of post-disaster loss and reconstruction demand in an  
 205 impacted region. Previous applications of the ARIO model typically assigned this reconstruction demand  
 206 to the real estate sector (Hallegatte 2014; Markhvida and Baker 2023). While this approach accounts for  
 207 housing loss in the analysis, it treats their replacement costs as productive capital. Since the ARIO model  
 208 uses the ratio of loss to productive capital to estimate the initial drop in production, this approach can distort  
 209 economic recovery for the real estate sector and cause unintended upstream and downstream ripple effects.

210 Rather than assigning housing losses and productive capital to an individual sector, the improved R-ARIO  
 211 approach assigns housing losses to a distinct housing "sector." This sector only generates reconstruction

212 demands, and is assumed to hold no productive capital. The housing sector does not contribute to any  
213 macroeconomic calculations of inputs, outputs, or production. With this treatment, it is accounted for in the  
214 analysis without influencing the initial drop in production for non-housing sectors.

### 215 **Sector-level behavioral parameter modeling**

216 Finally, the R-ARIO model utilizes sector-level behavioral parameter modeling to enable more gran-  
217 ular refinement, uncertainty quantification, and global sensitivity analysis. Behavioral parameters, which  
218 characterize sector-level adaptation and inventory mechanics, significantly influence the predicted economic  
219 recovery and indirect loss. For example, past sensitivity analyses have shown that the choice of inventory  
220 parameters  $n_s$  and  $\tau_s$  can move predicted changes in value added shortly after the disaster from moderate (<  
221 20%) to economic collapse (100%) (Hallegatte 2014).

222 The R-ARIO model considers the same five ARIO behavioral parameters that control economic recovery  
223 dynamics. Time to maximum overproduction ( $\tau_\alpha$ ) introduces a temporal dimension, defining the duration  
224 needed for the production system to adjust and reach peak overproduction capacity. Time of inventory  
225 restoration ( $\tau_s$ ) quantifies the duration required to restore inventory levels to the predefined target after  
226 a disruption. The maximum overproduction parameter ( $\alpha_{max}$ ) defines the upper limit of overproduction  
227 capacity in response to increased demand. Target inventory level ( $n_j$ ) represents the temporal dimension  
228 of inventory management, specifying the duration for which available inventory can support production.  
229 Finally, the production reduction (or heterogeneity) parameter ( $\psi$ ) captures the response of businesses to  
230 disaster impacts, influencing the extent to which production is reduced when inventories are insufficient.

231 Past studies (e.g. Ranger et al. 2011; Zhang et al. 2017; Wang et al. 2018; Liu et al. 2023; Markhvida  
232 and Baker 2023) assign identical parameter values for each sector in the economy, typically using the values  
233 proposed by Hallegatte (2014) and indicated in Figure 3. An exception to this is for sectors with non-stockable  
234 goods — in those cases, the target inventory level  $n_j$  is set to 3 days to account for the fact that many sectors  
235 cannot store long-lasting inventories (e.g., utilities).

236 The R-ARIO model includes updated behavioral parameters split across seven major sector categories  
237 (Figure 3). This proposed set retains some prior values and makes amendments where evidence is available.  
238 Furthermore, we maintain treatment for "non-stockable" goods for utilities sectors (Hallegatte 2014), as  
239 described earlier in this section. We use these parameters later as part of the case study.

240 For each category-parameter pair, we also define lower and upper bounds (denoted by the blue bars in

Figure 3) for use in uncertainty quantification and sensitivity studies. Hence, the parameter values selected serve as the central values of their corresponding sampling distribution.

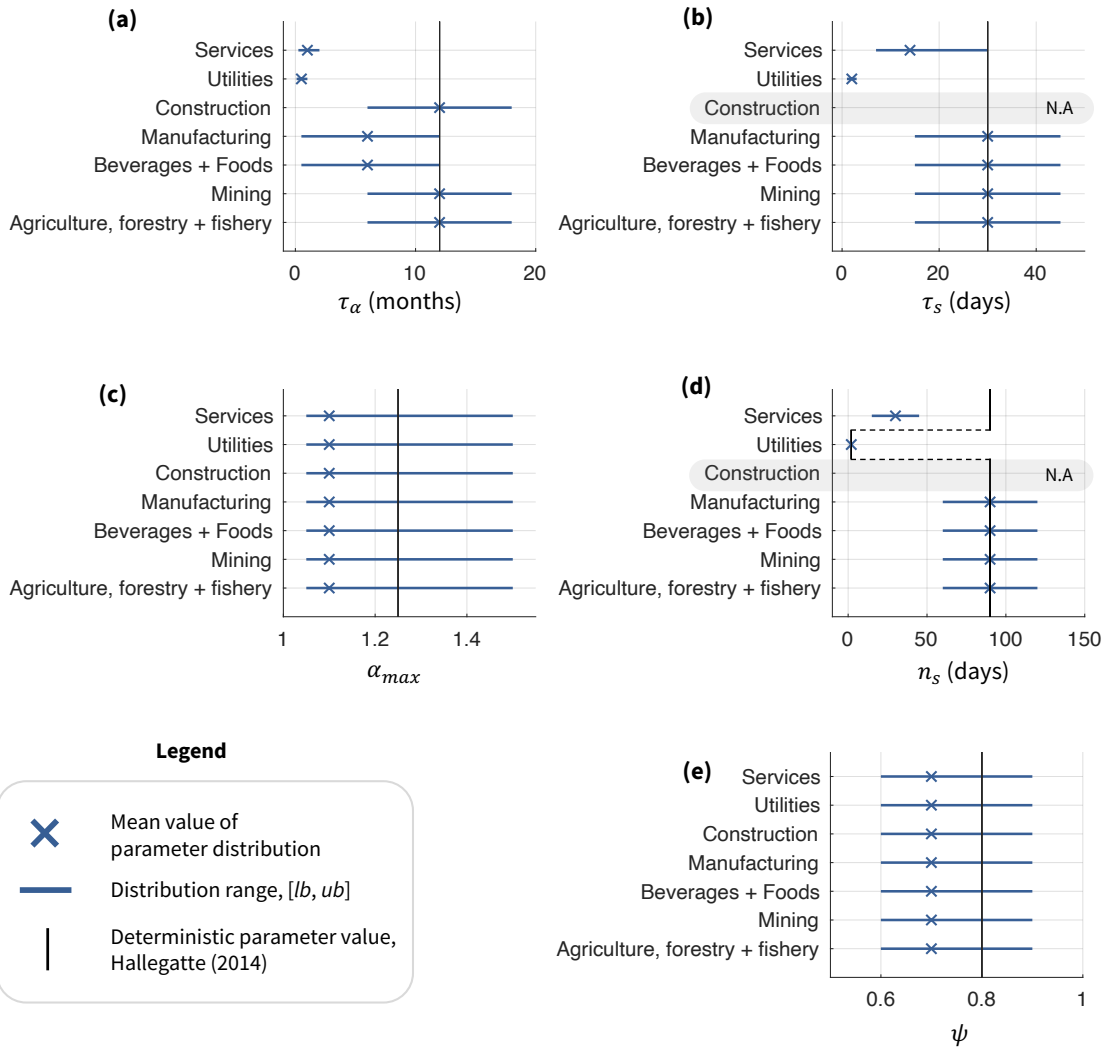


**Fig. 3.** Proposed distributions of behavioral parameters for each of the defined sector categories, compared against the default values in Hallegatte 2014.

243 *Overproduction parameters*

244 We refine overproduction parameters  $\tau_\alpha$  and  $\alpha_{max}$  (Figure 3a, Figure 3c). First, we reduce  $\tau_\alpha$  from 12  
 245 months to 6 months for Manufacturing and Beverages + Foods sectors, drawing insights from the accelerated  
 246 deployment of production recapture strategies following events like the 2016 Kumamoto Earthquake (S&P  
 247 Global 2016a; S&P Global 2016b; Maruya et al. 2017). We reduce  $\tau_\alpha$  from 12 months to 1 month for  
 248 Services sectors. Services typically carry little inventory compared to other sectors, and can adapt rapidly

249 due to high teleworking potential compared to non-services industries (OECD 2021). For Utilities sectors,  
250 where responsiveness to consumer demand is critical, we reduce  $\tau_\alpha$  to 3 days to reflect agility in adjusting  
251 production continuously to match demand, many times throughout the day (e.g., energy utilities). Finally,  
252 we lower  $\alpha_{max}$  from 125% to 110% across all sectors to better align with empirical industrial productivity  
253 indices (IIPs) following the 2011 Tohoku Earthquake (Kajitani et al. 2013; Ministry of Economy, Trade and  
254 Industry (METI) 2018).

### 255 *Inventory parameters*

256 In most cases, we maintain the default values of inventory parameters  $\tau_s$  and  $n_s$  (Figure 3b, Figure 3d),  
257 except for Utilities and Services sectors, where we reduce  $\tau_s$  from 30 days to 3 days. This implies that Utility  
258 sectors can rapidly replenish their inventories when productive capital remains undamaged. Similarly, for  
259 Services sectors, we reduce  $\tau_s$  from 30 days to 14 days to reflect rapid adaptability. Finally, we reduce  $n_s$   
260 from 90 days to 30 days for Services sectors, because Services sectors carry little inventory compared to  
261 other sectors.

### 262 *Heterogeneity parameter*

263 Finally, we reduce the heterogeneity parameter  $\psi$  from 0.8 to 0.7 for all sectors to reflect recent studies  
264 of post-shock substitutional elasticity (Figure 3e). Fujii et al. (2022) suggests that elasticities (the degree  
265 to which consumers or producers can switch between different goods or services in response to changes in  
266 prices or availability) are slightly higher (between 0.38 and 0.41) than previously reported in Atalay (2017).  
267 Such an increase implies that production reductions (that arise when inventories are insufficient) are softened,  
268 due to increased flexibility. As a result,  $\psi$  should decrease to reflect increased input substitutability.

## 269 **R-ARIO BEHAVIORAL PARAMETER SENSITIVITY ANALYSIS**

270 In this section, we describe a Sobol sensitivity analysis (Saltelli et al. 2010) to quantify the influence of  
271 R-ARIO behavioral parameters on the predicted indirect loss. We apply this approach for the parameters  
272 assigned to the  $N_{cat} = 7$  sector categories defined in Figure 3.

273 First, we select sampling bounds for the behavioral parameters based on the upper and lower bounds in  
274 Figure 3. Sobol sampling is used to efficiently cover the sample space.

275 Next, we generate samples of the behavioral parameters. Each sample of parameters  $\mathbf{X}^{(k)}$  is a  $N_{cat} \times 5$   
276 matrix, accounting for the five types of behavioral parameters:

$$\mathbf{X}^{(k)} = \begin{bmatrix} \psi_1^{(k)} & n_{s,1}^{(k)} & \tau_{s,1}^{(k)} & \alpha_{max,1}^{(k)} & \tau_{\alpha,1}^{(k)} \\ \psi_2^{(k)} & n_{s,2}^{(k)} & \tau_{s,2}^{(k)} & \alpha_{max,2}^{(k)} & \tau_{\alpha,2}^{(k)} \\ \vdots & \vdots & \vdots & \vdots & \vdots \\ \psi_{N_{cat}}^{(k)} & n_{s,N_{cat}}^{(k)} & \tau_{s,N_{cat}}^{(k)} & \alpha_{max,N_{cat}}^{(k)} & \tau_{\alpha,N_{cat}}^{(k)} \end{bmatrix} \quad (7)$$

where  $k$  is an index indicating the sample number, ranging from 1 to  $N_{sim}$ .

When using the proposed behavioral parameters introduced in the previous section,  $N_{cat} = 7$ , resulting in a total of 35 variables in the sensitivity analysis. For sample  $k$ , we run the R-ARIO model and record and the  $Loss$  (total indirect loss across the economy).

Using the ensemble of  $N_{sim}$  samples along with the recorded output, we estimate Sobol indices  $S_{1,i}$  and  $S_{T,i}$  for each of the  $N_{cat} \times 5$  variables. Each index uses an  $i$  subscript to denote one of the 35 variables in the analysis (e.g.,  $\alpha_{max}$  for the Manufacturing category).

$S_{1,i}$ , the first-order Sobol index, measures the contribution in output variance associated with modifying a variable in isolation:

$$S_{1,i} = \frac{\text{Var}[\mathbb{E}_{\mathbf{X}_{\sim i}}[Loss|X_i]]}{\text{Var}[Loss]} \quad (8)$$

where  $X_i$  is R-ARIO behavioral parameter variable  $i$  (associated with a specific parameter-category pair) and  $\mathbf{X}_{\sim i}$  denotes the set of all variables except  $X_i$ .

$S_{T,i}$ , the total-order Sobol index, measures a variable's first- and higher-order influence on predicting the model output. Unlike  $S_{1,i}$ ,  $S_{T,i}$  measures higher (or total-order) influence that accounts for all levels of interaction:

$$S_{T,i} = \frac{\mathbb{E}_{\mathbf{X}_{\sim i}}[\text{Var}_{X_i}[Loss|\mathbf{X}_{\sim i}]]}{\text{Var}[Loss]} \quad (9)$$

The inequality  $0 \leq S_{1,i} \leq S_{T,i} \leq 1$  must hold for all cases, in addition to:

$$\sum_i S_{1,i} < 1 \quad (10)$$

Finally, we use values of  $S_{1,i}$  and  $S_{T,i}$  to rank each variable. Any variables that heavily influence indirect losses will have high index values. Such variables should be prioritized for subsequent behavioral parameter refinement efforts.

299 It is important to note that variables at the sector category level are used here and in the case study to  
300 illustrate this method. Sector-level analyses can be obtained by expanding  $\mathbf{X}^{(k)}$  to consider  $N_s \times 5$  variables,  
301 where  $N_s$  is the number of sectors.

## 302 CASE STUDY: 2016 KUMAMOTO EARTHQUAKE

303 An analysis of the 2016 Kumamoto Earthquakes in Japan is used here to demonstrate the R-ARIO model,  
304 identify key drivers of indirect loss, and compare predicted recovery times obtained from variants of the  
305 model. We begin with an overview of the study region and disaster, followed by a summary of model inputs,  
306 implementation, and analysis results. Finally, we discuss the application of a variance-based sensitivity  
307 analysis on the selected behavioral parameters.

### 308 Overview of study region and disaster

309 Located in the southern island of Kyushu in Japan, Kumamoto is one of the country's 47 prefectures and  
310 home to 1.3% of its population. The capital, Kumamoto City, is home to over 40% of the prefecture's 1.7  
311 million population (Figure 4), and serves as a key economic hub. Kumamoto's 2016 GDP was roughly 6  
trillion yen, just over 1% of Japan's GDP.

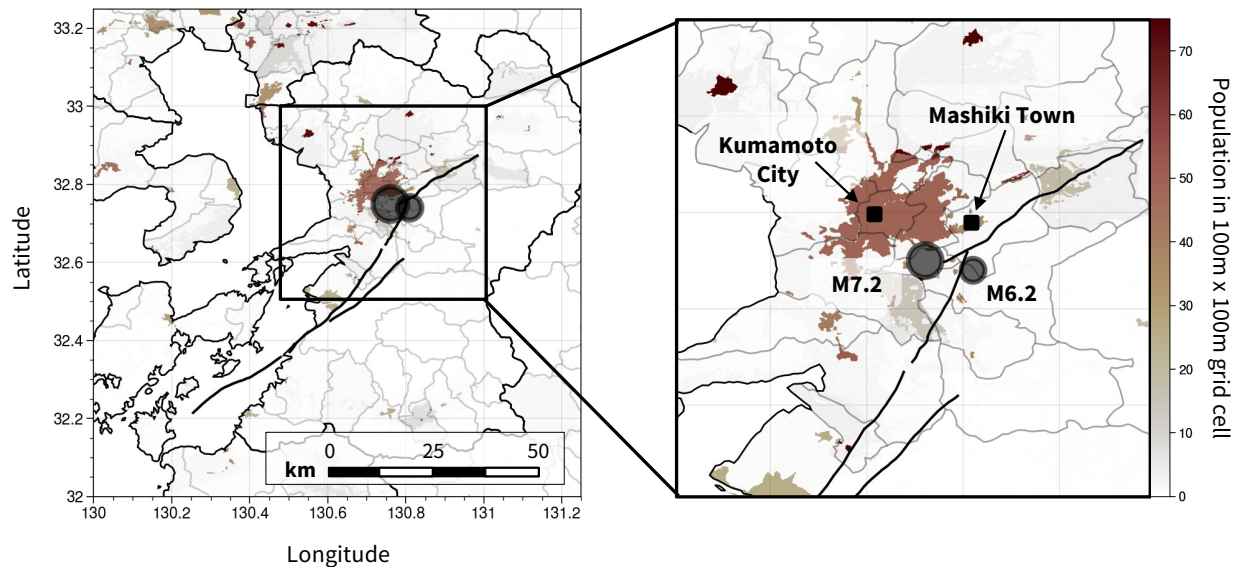


**Fig. 4.** Epicenters of major earthquakes (indicated by circles) and population density in the Kumamoto Prefecture (indicated by shading), along with fault traces for the Futagawa-Hinagu fault zone.

312 The Kumamoto Earthquake sequence occurred along the Futgawa-Hinahgu fault in the Kumamoto  
313 prefecture, beginning with a  $M_w$  6.2 foreshock on April 14th, followed by a  $M_w$  7.0 mainshock two days  
314

315 later. Multiple significant aftershocks in the following days caused additional destruction. Damage and  
316 fatalities from the foreshock were concentrated in Mashiki Town, a small suburb north of the fault zone. The  
317 mainshock exacerbated the damage in Mashiki and extended the radius of influence to nearby Kumamoto  
318 City. Two hundred seventy-three confirmed casualties have been reported (Kumamoto Cabinet Office 2016).

319 Over 198,000 homes in the prefecture experienced some form of damage, with over 20% experiencing  
320 collapse (Kumamoto Prefecture 2022). As a result, over 60% of losses reported by the Office of the Cabinet  
321 stemmed from housing. Commerce and industrial assets sustained significant damages, causing cascading  
322 supply chain disruption across Japan. Damage to buildings and infrastructure in the prefecture produced  
323 losses of roughly 3.79 trillion yen as of September 14th, 2016 (Kumamoto Cabinet Office 2016).

### 324 **Assemble inputs**

325 Next, we describe the assembly of the necessary input data for the R-ARIO model (Table 1). This data  
326 falls into four categories: pre-disaster economic data, monetary losses due to direct damage, repair time  
327 curves, and ARIO behavioral parameters.

#### 328 *Pre-disaster economic data*

329 We assemble the input-output table and key economic metrics (e.g., value added, total final demand,  
330 exports, imports, and local demand) for Kumamoto from official prefectural data (Kumamoto Prefecture  
331 2020) for the 2015 fiscal year. The input-output table, consisting of 37 productive sectors, is visually  
332 represented in the electronic supplement, Figure S1. We compute sector-level fixed assets using replacement  
333 costs provided by Sompo Inc. (Table S1).

#### 334 *Direct losses*

335 We derive sector-specific direct losses by aggregating building-level claims data supplied by Sompo Inc  
336 (Table S2). Total building damage losses across all sectors are 1.76 trillion Yen, and further details regarding  
337 the treatment of losses can be found in the electronic supplement. We assume that 75% of reconstruction  
338 demand from these losses are distributed to the construction sector, and the remaining 25% are distributed  
339 to manufacturing sectors, consistent with past studies (e.g., Hallegatte 2008; Markhvida and Baker 2023)

#### 340 *Reconstruction time curves*

341 Sector-specific reconstruction time curves are used to determine the rate of reconstruction at each time  
342 step in the R-ARIO model. We develop each curve using building-level reconstruction times, which are  
343 estimated using a proprietary model by Sompo Inc. These times are strictly limited to repairs and do not



344 include impediments to reconstruction progress. Upon converting building-level reconstruction data into  
345 sector-level reconstruction trajectories, we observe that the time to 95% reconstruction is achieved within  
346 six months. Trajectories for each sector are illustrated in the electronic supplement, Figure S2.

### 347 *Behavioral parameters*

348 The proposed set of behavioral parameters in Figure 3 is employed for the case study. We tabulate  
349 assigned sector categories for each of the 37 productive sectors in the electronic supplement, Table S3.  
350 The impact of the refined set, relative to the default ARIO parameters introduced in Hallegatte (2014), is  
351 described in the next section.

### 352 **R-ARIO model results**

353 In this section, we describe the R-ARIO-predicted post-earthquake indirect loss, value added dynamics,  
354 and reconstruction over time at various resolutions. Next, we explore the influence of the R-ARIO model on  
355 recovery time and quantify the influence of the proposed behavioral parameters on predicted indirect loss.

#### 356 *Post-earthquake economic loss and recovery at the economy-level*

357 To examine the impact of the R-ARIO model refinements, we simulate regional economic recovery using  
358 several variants of the model, as listed below:

- 359 • **Dynamic Reconstruction + explicit Housing losses + Behavioral Parameter Refinement (DR+H+BPR):**  
360 this is the complete R-ARIO model proposed in this study.
- 361 • **Dynamic Reconstruction + explicit Housing losses (DR+H):** this is the R-ARIO model introduced  
362 in this paper, but it uses the Hallegatte (2014) behavioral parameters rather than the proposed refined  
363 sector-level behavioral parameters.
- 364 • **Baseline:** this is equivalent to the original ARIO model.

365 Indirect losses predicted by the DR+H+BPR model over the first 30 days amount to roughly 88 billion,  
366 which is within reported estimates by the Cabinet Office during the same period (81 to 113 billion yen). The  
367 DR+H and Baseline model predictions are also within this range, at 91 and 101 billion yen, respectively.  
368 Indirect loss estimates over an analysis period of five years following the earthquake, aggregated at the  
369 economy level, are shown in Figures 5c-e for each case, along with the associated post-earthquake dynamics  
370 in value added (Figure 5b), and productive capital recovery trajectory (Figure 5a).

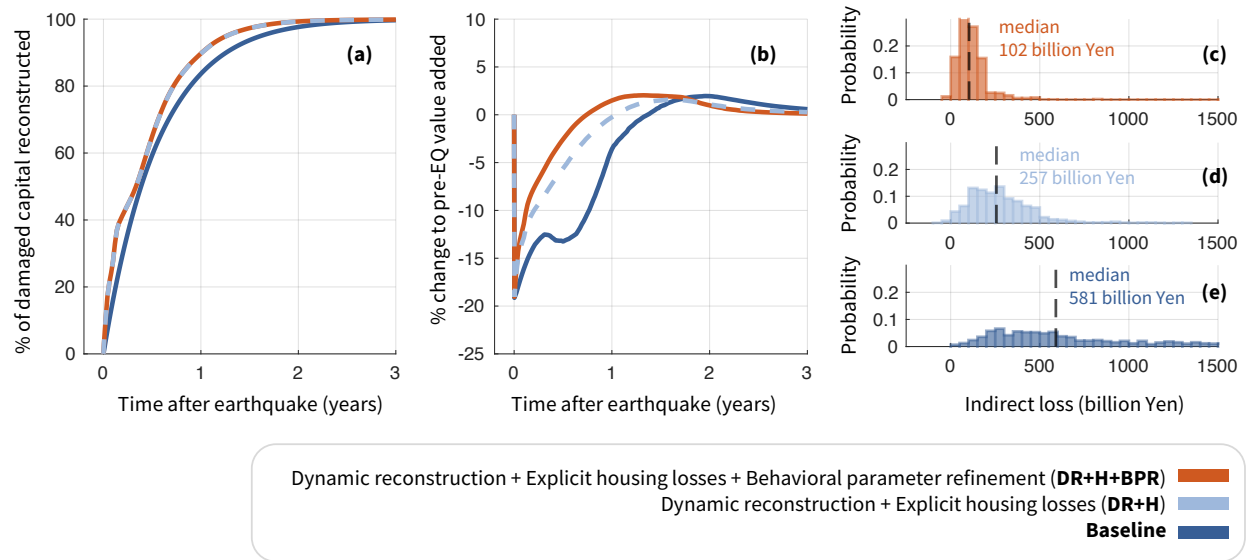


**Fig. 5.** Results for each of the three models explored in this case study, based on an ensemble of 1000 simulations and a recovery period of 5 years. Panels (a) and (b) represent the recovery of productive capital and value added, respectively, each taken at the 50th percentile. The histograms in (c), (d), and (e) illustrate the indirect losses across the ensemble for different variants of the R-ARIO model. Dashed lines indicate the 50th percentile value in each case.

371 Figure 5a shows the predicted capital recovery, accounting for economic constraints that impede repairs  
 372 of productive capital. Recovery is rapid during the first year following the disaster. The DR+H and  
 373 DR+H+BPR models — which both incorporate dynamic reconstruction — follow very similar trajectories  
 374 and exhibit higher rates of recovery, particularly in the first few months. Across all three models, more  
 375 than 50% of damaged capital recovers within the first six months of the initial shock, and 95% recovers  
 376 within 2 years. Both the DR and DR+BPR models predict a shorter time to 95% recovery of 1.25 years,  
 377 compared to 1.60 years for the Baseline model. The dynamic reconstruction assumption can account for the  
 378 swift progress made during the first month of recovery (reconstruction time curves for Kumamoto sectors  
 379 generally exhibited rapid reconstruction initially), while the baseline model is forced to leverage a constant  
 380 reconstruction rate that cannot capture this progress.

381 Figure 5b shows the recovery of value added. Each model predicts an equal initial 19% drop in prefectural  
 382 value added. Value added recovers rapidly in the first year and returns to pre-disaster values at 0.7, 1.0, and  
 383 1.5 years for the DR+H+BPR, DR+H, and Baseline models, respectively. Due to assumed overproduction,  
 384 value added continues to increase, with median trajectories peaking at 2.03, 2.00, and 1.59 percent of pre-  
 385 earthquake value added for the DR+H+BPR, Baseline and DR+H models, respectively. Beyond the peak,

386 value added descends and eventually converges to pre-disaster values. As observed with recovery times,  
387 DR+H+BPR peaks the quickest, followed by DR+H, and Baseline. Of the three models, the Baseline model  
388 is the only one to exhibit non-monotonic recovery due to supply-side constraints that impede recovery at  
389 around six months.

390 Figures 5c-e show the total predicted indirect loss over the analysis period. Each realization of value  
391 added can be integrated across time to obtain a corresponding realization of total indirect loss at the economy  
392 level. Of the three models, DR+H+BPR predicts the lowest median indirect loss over the entire recovery  
393 period, at roughly 102 billion yen. Without behavioral parameter refinement, the DR+H and Baseline model  
394 predict substantially higher median indirect losses of 257 billion yen and 581 billion yen, respectively.  
395 The significantly higher losses predicted by the DR+H and Baseline are due in part to longer  $\tau_\alpha$  values  
396 associated with the default ARIIO behavioral parameter settings. Notably, the significant median indirect  
397 loss predicted by the Baseline model is due to its much longer period of non-recovery compared to the other  
398 two models. Overall, including behavioral parameter refinement reduces the predicted median indirect loss  
399 over the recovery period by 155 billion yen when compared to the DR+H model (i.e., the difference between  
400 median losses in 5c and d).

#### 401 *Sector-level economic recovery*

402 The results in Figure 5 can be disaggregated by sector to reveal recovery attributes not visible at the  
403 aggregate economy level. For each sector, we extract building recovery, production capacity, production,  
404 demand, and value added over time. Figure 6 shows Construction sector results to demonstrate relationships  
405 between demand, production capacity, and value added over time. As part of this example, we examine the  
406 single realization associated with the median indirect loss shown in Figure 5.

407 Figure 6a shows that capital is nearly reconstructed within two years of the disaster. This resembles the  
408 economy-level productive capital recovery trajectory in Figure 5a.

409 Figure 6b shows trends in production and demand. Immediately following the disaster, demand for the  
410 Construction sector dramatically increases. This sharp increase in demand is expected because 75% of all  
411 reconstruction demand is assigned to the Construction sector. During this same period, the sector loses over  
412 20% of its pre-disaster production capacity, constraining production, and hence, ability to fulfill demand.  
413 Within 0.7 years, production capacity is restored to its pre-disaster level but is still unable to meet demand  
414 and begins moving into overproduction. An extra capacity equivalent to 20% of pre-disaster production is

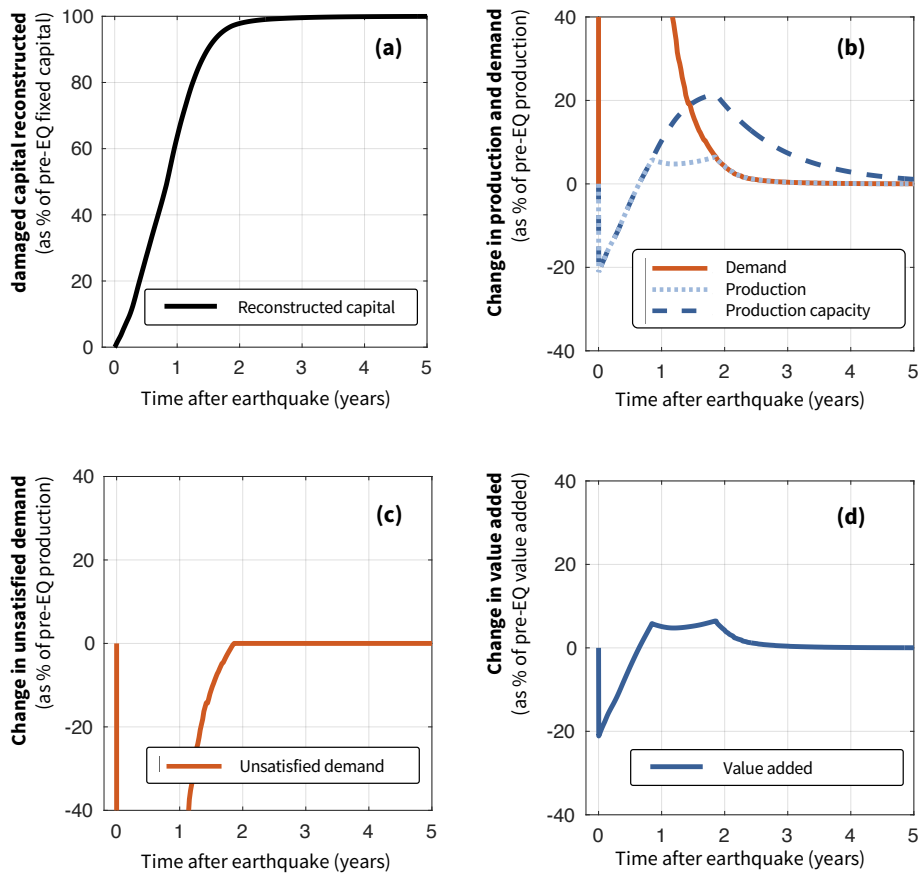


**Fig. 6.** Results for a single ARIO realization (associated with the 50th percentile indirect loss in Figure 5c) for the Construction sector.

415 gradually added to the sector roughly 1.6 years after the disaster. Interestingly, while capacity grows to reach  
 416 elevated demand, actual production (light blue curve) cannot keep up and production plateaus at roughly  
 417 5% over baseline production due to supply-side constraints. During this plateaued period of production,  
 418 demand is rapidly decaying and the Construction sector's actual production can fulfill all demand by year 2  
 419 (the orange and light blue curves merge). Demand returns to pre-earthquake levels (along with production)  
 420 shortly after. Production capacity, by comparison, is significantly slower to return to baseline.

421 Figure 6c shows the amount of unsatisfied demand (the difference between the demand and production  
 422 curves in Figure 6b) over the entire recovery period. By the end of the year 2, the demand unsatisfied returns  
 423 to 0, indicating that all demand can be fulfilled by production beyond this point.

424 Finally, the value added trajectory (Figure 6d) quantifies the changes in value added over time, and is

425 used to calculate the indirect losses of the sector (through integration of trajectory over the entire recovery  
 426 period). Value added takes the sharpest loss immediately following the disaster, decreasing by an amount  
 427 equivalent to over 20% of its pre-disaster value. Due to the rapid initiation of overproduction, value added  
 428 is restored to its pre-earthquake value added within 0.7 years of the initial drop. The time to recover value  
 429 added takes roughly 35% of the time to recover all physical capital shown in Figure 6a. This trend, whereby  
 430 sectors achieve quicker recovery of lost value added compared to recovery of damaged productive capital,  
 431 is observed for nearly all sectors in the Kumamoto economy. Value added peaks at roughly 0.8 years after  
 432 the earthquake, plateaus for an additional year, then gradually decreases to its pre-earthquake value before  
 433 year three. Other sector-specific trajectories, including uncertainty bounds, can be found in the electronic  
 434 supplement, Figures S4-S9.

435 *Sector-level losses*

436 We integrate sector-specific value added curves for each of the 37 sectors to quantify the absolute total  
 437 loss, and the losses as a fraction of the pre-earthquake value added, broken down by direct and indirect  
 438 sources. Results for each sector can be found in the electronic supplement, Figure S10. To simplify  
 439 presentation, we sum the sector-level 50th percentile indirect losses for each of the seven categories proposed  
 440 in Figure 3.

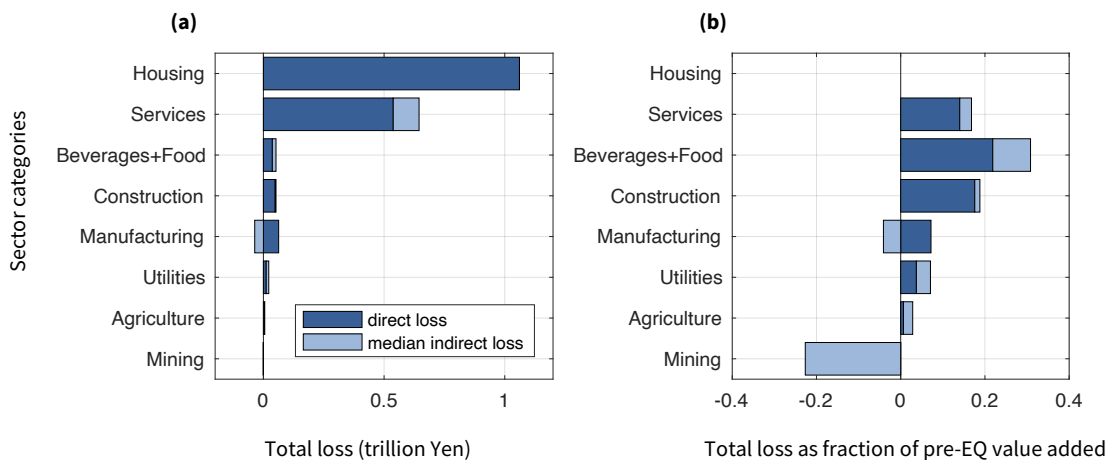


**Fig. 7.** 50th percentile direct and indirect losses across the seven economic sector categories (plus housing) in terms of absolute monetary value in trillion yen (left) and fraction of pre- disaster value added.

441 Figure 7 shows the direct and indirect losses per sector category, in absolute values and as a fraction  
 442 of the total value added across all sectors within a category. The 50th percentile indirect loss across the

443 economy (102 billion yen) is small relative to total losses (1.7 trillion yen). In absolute monetary terms,  
444 the Services category incurs the greatest indirect loss across all categories, followed by the Beverages +  
445 Food and Utilities categories. Interpreting these results within the context of the economic recovery yields  
446 a number of insights.

447 The Construction category's indirect loss (both in absolute terms and as a fraction of its pre-earthquake  
448 value added) is relatively low compared to other categories. This relatively small loss stems from the  
449 substantial gains due to overproduction (e.g., that of the kind observed in Figure 6b). Such overproduction  
450 is expected, since the demand for reconstruction following the disaster is substantial. When integrating the  
451 value added trajectory to obtain the indirect loss, the initial shock is barely significant enough to counteract  
452 large gains from overproduction.

453 The Manufacturing category (e.g., iron + steel, production machinery, plastic products + rubber products  
454 sectors) experiences a net gain in value added due to strong overproduction across several sectors, as 25% of  
455 the reconstruction demand goes to manufacturing sectors. Across a handful of Manufacturing sectors, the  
456 gain from overproduction counteracts the initial drop in value added.

457 The Mining category (which consists solely of the mining sector) also experiences a net gain in value  
458 added. This result is attributed to a gentle initial drop in value added, and a notably extended duration of  
459 overproduction. The mining sector is implicitly critical to the reconstruction of economic capital, since it  
460 is the primary supplier to the electricity, gas, and heat sector (within the utilities category), which supplies  
461 a significant number of manufacturing sectors (per the I-O table in the electronic supplement). The Mining  
462 category is among the few sectors to incur zero direct damage in the analysis inputs, which influences the  
463 observed net gain.

#### 464 *Influence of ARIO model on recovery time*

465 Previous sections illustrated how ARIO-predicted recovery in value added, production, and productive  
466 capital can be disaggregated at the individual sector level. These sector-level trajectories can be used to  
467 extract time-to-recovery statistics, such as the time to restore lost value added. Such measures can then be  
468 used to compare recovery performance across sectors. Figure 8 provides a comparison of time-to-recovery  
469 metrics for the seven sector categories, plus housing. All reported metrics are based on 50th percentile  
470 recovery trajectories across an ensemble of 1000 simulations. Times represented at the sector category level  
471 are estimated by averaging times across all sectors within a category.

472 For each sector, we extract the R-ARIO-predicted times to recover 95% of the lost value added, production,  
 473 and productive capital. Across most categories, the median value added is restored to pre-earthquake levels  
 474 within one year. The Manufacturing and Agriculture categories are the quickest and slowest to recover, at  
 475 0.5 and 1.2 years, respectively. Recovery of production is nearly identical to that of value added across  
 476 all categories. Times to recover value added and production for housing are set to zero in Figure 8, since  
 477 housing is not a productive sector.

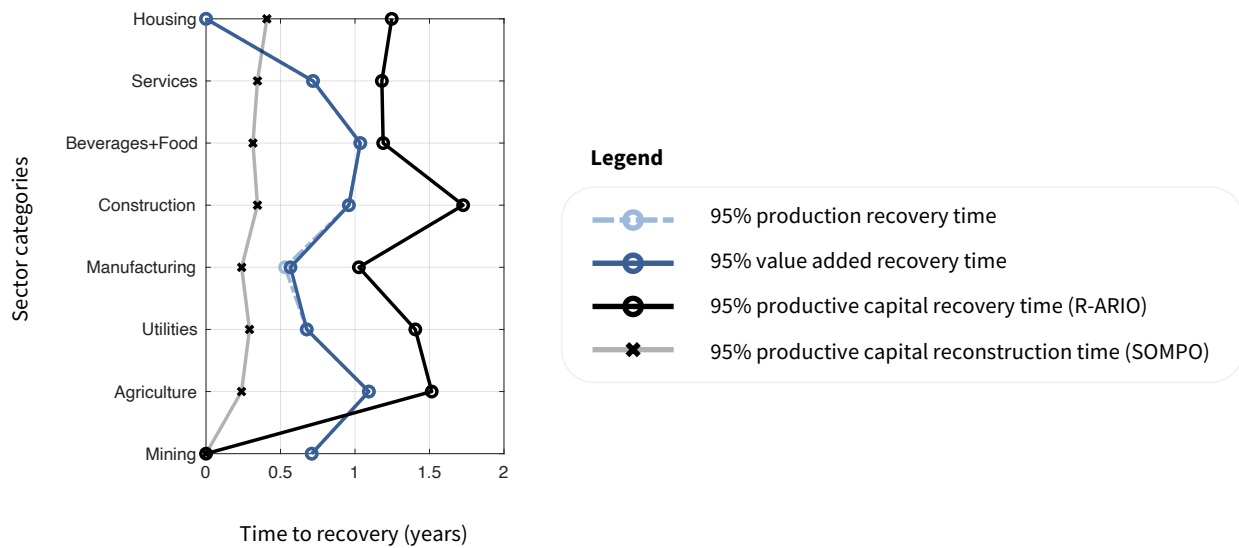


**Fig. 8.** R-ARIO-predicted time to recover 95% of lost production, R-ARIO-predicted time to recover 95% of lost value added, R-ARIO-predicted time to recover 95% of damaged productive capital, and time to reconstruct 95% of damaged capital based on user-provided reconstruction time curves. In all four cases, sector category averages are shown.

478 The R-ARIO-predicted time to recover 95% of damaged productive capital accounts for supply and  
 479 reconstruction constraints. Across all sector categories with damaged capital (i.e., not the Mining category),  
 480 Manufacturing sectors experience the swiftest recovery of productive assets on average, at roughly one year.

481 The reconstruction time data used to generate reconstruction time curves (and hence, the dynamic recon-  
 482 struction rates used in the R-ARIO model for individual sectors) is generated using a proprietary catastrophe  
 483 model by Sompo Inc. While these repair time curves are useful for enabling dynamic reconstruction rates,  
 484 they do not take into account supply chain disruptions, or the capacity of the construction sector to fulfill  
 485 post-disaster reconstruction demand. Past studies, such as [Markhvida and Baker \(2023\)](#), have demonstrated  
 486 that the resulting sector- and community-level repair times generated by similar models (e.g., HAZUS ([Fed-](#)

487 [eral Emergency Management Agency \(FEMA\) 2020](#))) can be significantly lower than the recovery time  
 488 estimates made by the ARIO model.

489 Figure 8 compares R-ARIO-predicted productive capital recovery times and Somp-provided recon-  
 490 struction times. The average time to repair 95% of damaged capital is 0.28 years, per Somp-provided  
 491 reconstruction time data (which do not include supply or reconstruction delays). The R-ARIO model pre-  
 492 dicts significantly longer average recovery times, at 1.1 years. The longer estimate provided by the R-ARIO  
 493 model is consistent with documented reports of capital recovery, particularly housing. One year after the  
 494 Kumamoto Earthquake, thousands of households were still residing in temporary housing ([Takeda and Inaba](#)  
 495 [2022](#)).

496 **ARIO model parameter sensitivity**

497 Next, we perform a Sobol sensitivity analysis to understand the relative importance of sector-specific  
 498 behavioral parameters on the predicted indirect losses shown in Figure 5. We compute  $S_{1,i}$  and  $S_{T,i}$  using  
 499 equations 8 and 9, respectively. The results, displayed in Figure 9, show several features of the analysis.  
 500 The behavioral parameter variables relating to inventory (particularly  $n_s$ ) significantly influence the indirect  
 501 losses. While this finding is consistent with the ARIO sensitivity studies in [Markhvida and Baker \(2023\)](#)  
 502 and [Hallegatte \(2014\)](#), our results unveil new sector-specific insights.

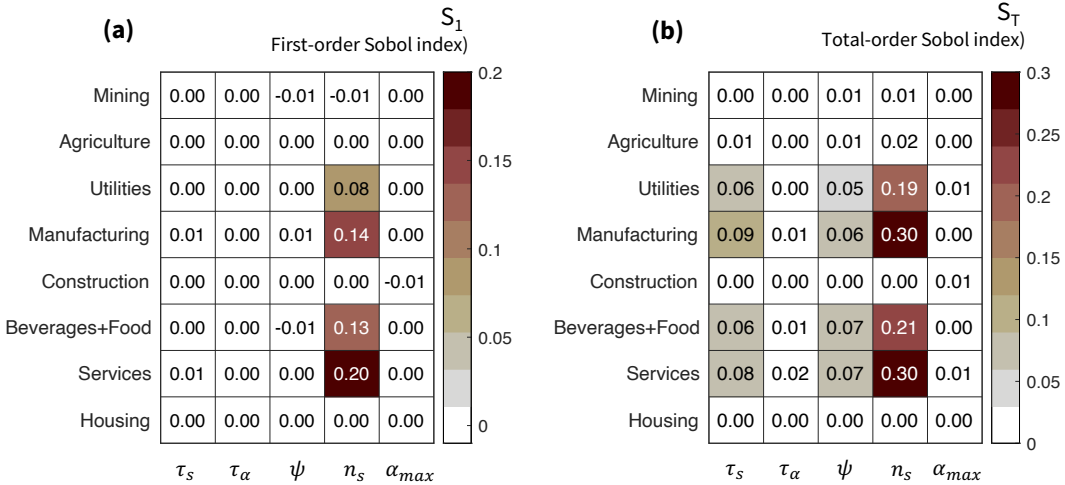


**Fig. 9.** (a) First-, and (b) total-order Sobol indices across the seven sector categories and behavioral parameters, measured with respect to the R-ARIO-predicted indirect loss across the prefecture.

503 Figure 9a shows that not all category-specific behavioral parameter variables for  $n_s$  exhibit the same  
 504 modeling importance. For example, the  $n_s$  parameter variables for Manufacturing, Services, and Beverages



505 + Food sectors are significantly more important than for those of other categories, and explain 20%, 14%,  
506 and 13% of the total first-order variance of the indirect loss, respectively.

507 When higher order effects are considered (Figure 9b), the importance of  $n_s$  holds, and sector category  
508 rankings based on  $S_{1,i}$  hold true for  $S_{T,i}$ . Interestingly, inventory parameter  $\tau_s$  and heterogeneity parameter  
509  $\psi$ , which have near-zero first-order indices, have more significant  $S_{T,i}$  values. Similar to  $n_s$ , both  $\tau_s$  and  $\psi$   
510 parameter settings for Manufacturing, Services, and Beverages + Food sectors have high importance. The  
511  $\tau_s$  parameters yield slightly higher  $S_{T,i}$  values than  $\psi$  in most cases.

512 Across 35 variables in this analysis, the top 3 variables when ranked using first- and total-order indices  
513 are associated with the  $n_s$  behavioral parameter. Across all settings of  $n_s$ , the value assigned to Services  
514 category is the most significant in both first- and total-order contexts. While this result motivated our careful  
515 scrutiny of the  $n_s$  parameter for the Services category, the results in this section suggest that priority for  
516 future refinements should be considered for the Manufacturing and Beverages + Food categories as well.

## 517 CONCLUSIONS

518 This paper presented R-ARIO, a refined ARIO model to simulate post-disaster economic recovery. The  
519 R-ARIO model incorporates (i) explicit modeling of housing losses separate from productive capital losses,  
520 (ii) dynamic reconstruction rates based on sector-specific reconstruction time curves, and (iii) sector-level  
521 modeling of behavioral parameters. The enhancements aim to improve indirect loss estimation, capture  
522 temporal differences in reconstruction demand, and enable uncertainty quantification, sensitivity studies,  
523 and refinement at the sector level.

524 We proposed a refined set of parameters across seven sector categories that address inter-sector dif-  
525 ferences, in accordance with available empirical observation and recent studies on post-disaster business  
526 adaptation. These parameters reflect inter-sector differences and can accommodate context-specific changes  
527 based on new evidence.

528 We used a global sensitivity analysis to evaluate the relative importance of specific behavioral parameters  
529 at the sector category level and guide subsequent refinement of the most influential parameters. Parameter  
530 bounds and a parameter sampling procedure are selected. An ensemble of simulated behavioral parameters  
531 is then generated, along with R-ARIO model outputs for each sample. Finally, Sobol indices are generated  
532 for each category-parameter pair to indicate the most influential sector-parameter pairs and rule out variables  
533 with negligible influence.

534 We applied the R-ARIO model to explore economic recovery following the 2016 Kumamoto Earthquake  
535 in Japan. Indirect losses predicted by the R-ARIO model over the first 30 days following the disaster align  
536 closely with the 81 to 113 billion yen range estimated by the Cabinet Office. Over a longer five-year analysis  
537 period, the R-ARIO model predicts a median indirect loss of 102 billion yen. When sector-level behavioral  
538 parameter modeling is omitted (and older default parameters are used in place of the proposed set) this loss  
539 more than doubles to 257 billion yen. The dynamic reconstruction assumption is responsible for properly  
540 modeling the high rate of recovery within the first month following the disaster, which previous, constant  
541 reconstruction rate assumptions cannot capture. Furthermore, explicit and separate modeling of housing  
542 losses prevents distortion of economic recovery caused by injecting significant direct damage into the real  
543 estate sector.

544 Using the R-ARIO model, aggregate indirect losses amount to 5.4% of the median total (direct + indirect)  
545 loss of 1.86 trillion yen. We evaluated sector-level indirect loss estimates to unveil trends across specific  
546 sector categories. Overall, the Services category generated the largest portion of indirect losses in absolute  
547 monetary terms, followed by Beverages + Food and Utilities categories. The Construction category sees low  
548 indirect loss (as a fraction of pre-earthquake value added) following the earthquake due to the compensating  
549 effect of overproduction. On the other hand, the Manufacturing category and the Mining category both  
550 experience net gains in value added, due to strong overproduction to support reconstruction that counteracts  
551 initial sector-level shocks.

552 Next, we evaluated the economic and productive capital recovery times for each sector category. In  
553 most cases, the value added recovers within a year, with the Manufacturing category recovering the quickest  
554 (0.5 years on average) and Agriculture the slowest (1.2 years on average). The average time to recover lost  
555 production is nearly identical to the time to recover value added for all productive sector categories. When  
556 comparing R-ARIO-predicted times to restore lost productive capital with user-provided reconstruction time  
557 curves, we found that the R-ARIO model extends the average time to 95% recovery of productive capital  
558 (across all sector categories) from 3.5 months to 13.5 months. The longer estimate provided by the R-ARIO  
559 model, which includes supply chain impacts that impede repairs, is more consistent with documented reports  
560 of recovery, particularly housing.

561 Finally, we applied the proposed sensitivity analysis approach to the Kumamoto case study. Sobol indices  
562 were generated for the 35 variables (representing behavioral parameter - sector category pairings) considered  
563 in the analysis. The inventory parameter  $n_s$  for Manufacturing, Services and Beverages+Food categories

564 explains 20%, 14%, and 13% of the total first-order variance in predicted indirect losses, respectively. These  
565 trends hold for the total-order variance as well. While inventory parameters are most important overall, there  
566 is significant variability in importance between categories. Therefore, efforts to refine behavioral parameters  
567 should focus on the subset of variables with significant influence on indirect loss.

#### 568 **DATA AVAILABILITY STATEMENT**

569 Some or all data, models, or code that support the findings of this study are available from the corre-  
570 sponding author upon reasonable request. Source code for the R-ARIO implementation used in the study is  
571 available at [github.com/Omarissa/SR-ARIO](https://github.com/Omarissa/SR-ARIO).

#### 572 **ACKNOWLEDGEMENTS**

573 We thank Sampo Holdings, Inc., including Mr. Ryu Saito, Mr. Shinji Yamada, and Mr. Katsuyoshi Sekii,  
574 for their support of this work, provision of data, and helpful feedback regarding our questions. This work  
575 was additionally supported by the National Science Foundation under NSF grant number CMMI-2053014  
576 and the Stanford Urban Resilience Initiative. Any opinions, findings, and conclusions or recommendations  
577 expressed in this material are those of the authors and do not necessarily reflect the views of Sampo Holdings,  
578 Inc. or the National Science Foundation.

#### 579 **SUPPLEMENTAL MATERIALS**

580 Figs. S1–10 and Tables S1-3, are available online as part of an electronic supplement in the ASCE  
581 Library ([ascelibrary.org](https://ascelibrary.org)).

## 582 REFERENCES

- 583 Atalay, E. (2017). “How Important Are Sectoral Shocks?.” *American Economic Journal: Macroeconomics*,  
584 9(4), 254–280 Publisher: American Economic Association.
- 585 Botzen, W. J. W., Deschenes, O., and Sanders, M. (2019). “The Economic Impacts of Natural Disasters:  
586 A Review of Models and Empirical Studies.” *Review of Environmental Economics and Policy*, 13(2),  
587 167–188.
- 588 Federal Emergency Management Agency (FEMA) (2020). “Hazus Earthquake Model Technical Manual.”  
589 *Report no.*, Washington, DC:.
- 590 Fujii, B. C., Ghose, D., and Khanna, G. (2022). “Production Networks and Firm-level Elasticities of  
591 Substitution.
- 592 Galbusera, L. and Giannopoulos, G. (2018). “On input-output economic models in disaster impact assess-  
593 ment.” *International Journal of Disaster Risk Reduction*, 30, 186–198.
- 594 Hallegatte, S. (2008). “An Adaptive Regional Input-Output Model and its Application to the Assessment of  
595 the Economic Cost of Katrina.” *Risk Analysis*, 28(3), 779–799.
- 596 Hallegatte, S. (2014). “Modeling the Role of Inventories and Heterogeneity in the Assessment of the  
597 Economic Costs of Natural Disasters: Modeling the Role of Inventories and Heterogeneity.” *Risk Analysis*,  
598 34(1), 152–167.
- 599 Haywired (2019). “Economic Consequences of the HayWired Scenario—Digital and Utility Network Link-  
600 ages and Resilience.” *Scientific Investigations Report*. Series: Scientific Investigations Report.
- 601 Kajitani, Y., Chang, S. E., and Tatano, H. (2013). “Economic Impacts of the 2011 Tohoku-Oki Earthquake  
602 and Tsunami.” *Earthquake Spectra*, 29(1\_suppl), 457–478.
- 603 Koks, E. E., Carrera, L., Jonkeren, O., Aerts, J. C. J. H., Husby, T. G., Thissen, M., Standardi, G., and Mysiak,  
604 J. (2016). “Regional disaster impact analysis: comparing input–output and computable general equilibrium  
605 models.” *Natural Hazards and Earth System Sciences*, 16(8), 1911–1924 Publisher: Copernicus GmbH.
- 606 Kumamoto Cabinet Office (2016). “Digital Archives of Kumamoto Disasters, <[https://www.kumamoto-  
608 archive.jp/en/about](https://www.kumamoto-<br/>607 archive.jp/en/about)>.
- 608 Kumamoto Prefecture (2020). “Kumamoto Prefecture Industry Association Table - Kumamoto Prefecture  
609 Homepage, <<https://www.pref.kumamoto.jp/soshiki/20/50333.html>>.
- 610 Kumamoto Prefecture (2022). “Damage from the Kumamoto Earthquake [Report 326].” *Report no.*,

611 <<https://www.pref.kumamoto.jp/uploaded/attachment/242582.pdf>>.

612 Liu, Y., Li, Y., Wang, G., Gao, G., and Chen, Y. (2023). “Quantifying multi-regional indirect economic  
613 losses: An assessment based on the 2021 rainstorm events in China.” *Frontiers in Earth Science*, 10,  
614 1057430.

615 MacKenzie, C. A., Santos, J. R., and Barker, K. (2012). “Measuring changes in international production from  
616 a disruption: Case study of the Japanese earthquake and tsunami.” *International Journal of Production  
617 Economics*, 138(2), 293–302.

618 Markhvida, M. and Baker, J. W. (2023). “Modeling future economic costs and interdependent industry  
619 recovery after earthquakes.” *Earthquake Spectra*, 1–24.

620 Maruya, H., Torayashiki, T., and International Research Institute of Disaster Science, Tohoku University  
621 468-1 Aramaki-Aza-Aoba, Aoba, Sendai, Miyagi 980-0845, Japan (2017). “Damage of Enterprises and  
622 Their Business Continuity in the 2016 Kumamoto Earthquake.” *Journal of Disaster Research*, 12(sp),  
623 688–695.

Ministry of Economy, Trade and Industry (METI) (2018). “Historical Data, Indices of Industrial Production,  
<<https://www.meti.go.jp/english/statistics/tyo/iip/b2010,result-2.html>>.

624 OECD (2021). “Measuring telework in the COVID-19 pandemic.” *OECD Digital Economy Papers 314* (July).  
625 Series: OECD Digital Economy Papers Volume: 314.

626 Petak, W. J. and Elahi, S. (2000). “The Northridge Earthquake, USA and its economic and social impacts.”  
627 IIASA, Laxenburg Austria (July).

628 Ranger, N., Hallegatte, S., Bhattacharya, S., Bachu, M., Priya, S., Dhore, K., Rafique, F., Mathur, P., Naville,  
629 N., Henriot, F., Herweijer, C., Pohit, S., and Corfee-Morlot, J. (2011). “An assessment of the potential impact  
630 of climate change on flood risk in Mumbai.” *Climatic Change*, 104(1), 139–167.

631 Rose, A. and Liao, S.-Y. (2005). “Modeling Regional Economic Resilience to Disasters: A Computable General  
632 Equilibrium Analysis of Water Service Disruptions\*.” *Journal of Regional Science*, 45(1), 75–112.

633 Saltelli, A., Annoni, P., Azzini, I., Campolongo, F., Ratto, M., and Tarantola, S. (2010). “Variance based  
634 sensitivity analysis of model output. Design and estimator for the total sensitivity index.” *Computer Physics  
635 Communications*, 181(2), 259–270.

636 S&P Global (2016a). “Japanese production recovers in aftermath of Kumamoto earthquake; IHS fore-  
637 casts full recovery to take until Q4.” *S&P Global*, <[https://www.spglobal.com/mobility/en/research-  
638 analysis/japanese-production-recovers-in-aftermath-of-kumamoto-earthquake-ihs-forecasts-full-recovery-](https://www.spglobal.com/mobility/en/research-analysis/japanese-production-recovers-in-aftermath-of-kumamoto-earthquake-ihs-forecasts-full-recovery-)

639 to-take-until-q4.html> (April).

640 S&P Global (2016b). “S&P Global: Japanese vehicle output rises 1.7% y/y during May, exports up 4.6%  
641 y/y.” *S&P Global*, <[https://www.spglobal.com/mobility/en/research-analysis/japanese-vehicle-output-rises-  
642 17-yy-during-may-exports-up-46-yy.html](https://www.spglobal.com/mobility/en/research-analysis/japanese-vehicle-output-rises-17-yy-during-may-exports-up-46-yy.html)> (June).

643 Takeda, K. and Inaba, K. (2022). “The damage and reconstruction of the Kumamoto earthquake: an analysis  
644 on the impact of changes in expenditures with multi-regional input–output table for Kumamoto Prefecture.”  
645 *Journal of Economic Structures*, 11(1), 20.

646 Wang, C., Wu, J., He, X., Ye, M., and Liu, Y. (2018). “Quantifying the spatial ripple effect of the Bohai Sea ice  
647 disaster in the winter of 2009/2010 in 31 provinces of China.” *Geomatics, Natural Hazards and Risk*, 9(1),  
648 986–1005.

649 Wei, D., Chen, Z., and Rose, A. (2020). “Evaluating the role of resilience in reducing economic losses from  
650 disasters: A multi-regional analysis of a seaport disruption.” *Papers in Regional Science*, 99(6), 1691–1722  
651 \_eprint: <https://onlinelibrary.wiley.com/doi/pdf/10.1111/pirs.12553>.

652 Wein, A. and Rose, A. (2011). “Economic Resilience Lessons from the ShakeOut Earthquake Scenario.”  
653 *Earthquake Spectra*, 27(2), 559–573.

654 Wu, J., Li, N., Hallegatte, S., Shi, P., Hu, A., and Liu, X. (2012). “Regional indirect economic impact evaluation  
655 of the 2008 Wenchuan Earthquake.” *Environmental Earth Sciences*, 65(1), 161–172.

656 Zhang, Z., Li, N., Xie, W., Liu, Y., Feng, J., Chen, X., and Liu, L. (2017). “Assessment of the ripple effects and  
657 spatial heterogeneity of total losses in the capital of China after a great catastrophic shock.” *Natural Hazards  
658 and Earth System Sciences*, 17(3), 367–379.